



Non-destructive Weight Prediction Model of Spherical Fruits and Vegetables using U-Net Image Segmentation and Machine Learning Methods

Savaş Koç^{a*}, Halil Kayra^a

^aBatman University, Department of Mechanical Engineering, Batman, TURKEY

ARTICLE INFO

Research Article

Corresponding Author: Savaş Koç, E-mail: savas.koc@batman.edu.tr

Received: 10 February 2024 / Revised: 14 May 2024 / Accepted: 21 May 2024 / Online: 22 October 2024

Cite this article

Koç S, Kayra H (2024). Non-destructive Weight Prediction Model of Spherical Fruits and Vegetables using U-Net Image Segmentation and Machine Learning Methods. *Journal of Agricultural Sciences (Tarim Bilimleri Dergisi)*, 30(4):735-747. DOI: 10.15832/ankutbd.1434767

ABSTRACT

Artificial intelligence has become increasingly prominent in agriculture and other fields. Prediction of body weight in animals and plants has been done by humans using many different methods and observations from the past to the present. Although there has been extensive research on predicting the live body weight of animals, weight prediction of vegetables and fruits is not widely. As spherical or round-shaped fruits and vegetables are sold by weighing in the fields, markets and greengrocers, it is important to make weight predictions. Based on this, a model was developed to predict the weight of fruits and vegetables such as watermelons, melons, apples, oranges and tomatoes with the data obtained from their images. The fruit and vegetable weights were predicted by regression models using data obtained from images

segmented by the U-Net architecture. Machine learning models such as Multi-Layer Perceptron (MLP), Random Forest (RF), Decision Trees (DT), Support Vector Machines (SVM), Linear and Stochastic Gradient Descent (SGD) regression models were used for weight predictions. The most effective regression models are the RF and DT models. For regression training, the best success rates were calculated as 0.9112 for watermelon, 0.9944 for apple, 0.9989 for tomato and 0.9996 for orange. In addition, the results were evaluated by comparing them to the studies of weight prediction. The weight prediction model will help to sell round-shaped fruits and vegetables in the fields, markets and gardens using the weight predictions from the images. It is also a guideline for studies that follow the growth of fruit and vegetables according to their weight.

Keywords: Artificial intelligence techniques, image segmentation, Fruits and vegetables, Weight prediction

1. Introduction

The development of a country's economy is significantly reliant on the progress of its agricultural sector, which serves as a crucial source of employment for the poor (Gondchawar & Kavitar 2016). The demand for innovative approaches is increasing day by day in order to prevent the decrease in yield caused by problems such as climate change, food quality and safety, and post-harvest deterioration in the agricultural industry (Pathan et al. 2020). The implementation of smart technologies in agriculture has led to increased agricultural productivity and opened up new employment opportunities while reducing the need for manual labor (Barbole et al. 2021). Smart agriculture utilizes information and communication technologies to enhance the productivity and quality of agricultural produce. Precision agriculture is a field within smart agriculture that is part of the third agricultural revolution. This approach offers a more objective and precise means of analysis (O'grady et al. 2019).

Smart agriculture is a system incorporating applications that leverage science, innovation, and space technologies. The Internet of Things (IoT) is used for measuring soil quality, moisture levels and weather conditions (Friha et al. 2021). Additionally, various technologies including cloud communication, robotics, wireless sensor technologies, Unmanned Aerial Vehicles (UAVs), mobile devices, and Global Positioning System (GPS) are being used. The recent technological advancements have also led to an increase in Artificial Intelligence (AI) research (Kassim 2020). AI tools, such as Artificial Neural Networks (ANN), Fuzzy Logic used by Cornelis et al. (2006), Genetic Algorithms, Machine Learning used by Mahesh (2020) and Deep Learning used by Fernandes et al. (2020) are being used in areas such as agricultural production, medical science, health services, speech recognition, robotics and disease detection. When dealing with limited data, regression and classification can be performed using machine learning models such as Partial Least Squares (PLS) as used by Yan et al. (2019), ANN as used by Akkol et al. (2017), random forests as used by Babajide et al. (2020), and Support Vector Machines (SVM) as used by Faisal et al. (2020). Similarly, deep learning models such as Convolutional Neural Networks (CNN) used by Alzubaidi et al. (2021), Recurrent Neural Networks (RNN) used by Xiao & Zhou (2020), and Long Short-Term Memory (LSTM) used by Yu et al. (2019) are utilized in the big data applications. The most prevalent architectures employed for image segmentation include U-Net, Seg-Net, Mask R-CNN, FCN, and Deeplabv3, among others (Li et al. 2017; Rudenko et al. 2020). U-Net-based models,

which are successful in creating accurate mappings and processing small datasets, have been integrated into agriculture to extract multi-scale features for the segmentation of images with complex backgrounds. This approach has been successfully applied to fruit segmentation, resulting in more efficient object detection (Chicchón Apaza et al. 2020).

Studies on live weight estimations in animals and vegetables and fruits have been increasing recently compared to previous years. In the first studies, predictions were made using the data obtained from the body measurements of the animals, while recently, because animals are discomforted from contact data are created using the body measurements of the animals from the images using computer vision. With the development of artificial intelligence, the weight predictions are made by using both images and data obtained from sensors that monitor the development of plants in order to follow the development of animals and vegetables-fruits. Computer vision-based segmentation techniques are investigated to identify defective areas in fruits such as apples and bananas, and vegetables such as potatoes, tomatoes, and cucumbers (Rozario et al. 2016). 2D, 3D, and infrared cameras, computer image processing technologies, machine learning and deep learning algorithms are used for weight prediction models with complex levels (Ozkaya 2013). Data generation in these models is by extraction and selection of features, image selection, image segmentation, and digital images. Deep learning methods are more advantageous compared to traditional methods due to the complexity of the backgrounds and the presence of multiple objects in the animal images used for weight prediction.

Bargoti & Underwood (2024) used Watershed Segmentation (WS) and Circular Hough Transform (CHT) algorithms in the CNN and MLP-based apple detection study. They successfully identified the image of apples situated in close proximity to the apple image in the tree, which was obscured by leaves and branches. Similarly, Kang & Chen (2020) developed the Dual Attentive Fully Convolutional Siamese Networks (DasNet-v2) algorithm based on deep neural networks for visualizing the environment in which the apples in the tree are located. The apples in the tree were detected and segmented. Furthermore, Rudenko et al. (2020) concluded that segmentation success may be diminished when confronted with intricate images or a multitude of products within the same image. Naroui Rad et al. (2017) employed U-Net architectures, which have proven effective in image segmentation, to obtain data by proportioning the sizes of the products in the image.

In order to obtain new data, Kamiwaki & Fukuda (2024) calculated the volume, color and shape information of radish using 3D image analysis, while Jeong et al. (2024) measured the width and height of strawberries using a computer vision technique and a Light Detection and Ranging (LiDAR) sensor system. Duc et al. (2023) employed a digital image-based system to measure dimensions such as area, perimeter, length and width for soya beans. Xu et al. (2024), on the other hand, calculated the volumes of sweet potatoes with full surface imaging using a LiDAR sensor and a 3D machine vision system. In order to obtain new data for weight estimation, image-based systems such as digital imaging systems, LiDAR sensor systems, cameras, image processing, computer vision, as well as utilized agronomic and phenological factors of crops. Similarly, they are used in methods such as calculating the volume by immersion in water. Teoh & Syaifudin (2007) employed data comprising parameters such as chakan mango area, mango and plant height, and the number of crops in the image.

Xu et al. (2020) estimated the lowest cotton boll weight with a success rate of 81.70%. Kamiwaki & Fukuda (2024) achieved an accuracy rate of 95% in weight estimation for radishes using a RF model, which incorporated volume, color and shape information. Jeong et al. (2024) employed a camera and LiDAR sensor system to measure the size of strawberries, achieving a success rate of 95% with the help of a High-Resolution Networks (HRNet) neural network. Duc et al. (2023) achieved 98% accuracy with an RF model using area, perimeter, length and width measurements. Lee (2023) achieved an accuracy of 99.81% in predicting the weight of apples, bananas and oranges using the CNN model. Huynh et al. (2020) reported a success rate of 96.7% in estimating the weight of cucumbers using data obtained from images of carrots and cucumbers. Niyalala et al. (2019) achieved a 96.94% success rate with the Radial Basis Function (RBF)-SVM model by extracting features from deep images for the mass and volume prediction of cherry tomatoes. In a different study, Ying-Kai et al. (2023) employed an ANN model to predict weights of dragon fruit, utilizing new data such as pixel area, major and minor axis pixel length, obtained following the removal of noise and segmentation from the image using machine vision.

The weight of a single boll is considered an important criterion in determining the yield and quality of cotton. The weight of a cotton boll was estimated from multi-temporal high-resolution visible light remote sensing images acquired by a UAV. In this model, Fully Convolutional Networks (FNN) were used to detect bolls at the opening and extracting stages. Correlation analysis was performed by extracting Visible Band Difference Vegetation Index (VDVI) of during flowering, boll development and opening stages and the RGB mean values. The best results were obtained with least squares linear regression with $R^2= 0.8162$ and Back Propagation (BP) neural networks with $R^2= 0.8170$ (Xu et al. 2020). The weight estimation of the eggplant, data on agronomic and phenological factors such as plant height, number of fruits per plant, ratio of fruit length to fruit width, total yield and time to flowering were achieved using in the ANN. An accuracy of 93% was obtained using these parameters (Naroui Rad et al. 2017). Similarly, the weight estimation of melon is utilized a data set of phenological traits, including plant and fruit length, fruit width, number of fruits per plant, days to flowering, days to maturity, days to fruit formation, fruit cavity diameter, and fruit flesh diameter. RF and ANN were employed to predict the final fruit weight of melon, resulting in an accuracy of 88% with ANN (Rad et al. 2015). An ANN model was utilized to estimate the biomass weight of the Maccauba palm. The results were then compared to those obtained from a multiple-regression model. The success rate for dry weight predictions was 98%, while predictions for oil content decreased to 90% (Castro et al. 2017). To estimate the weight of the chokanan mango using image

processing and analysis methods, the pixels of the area covered by the mango in the image were calculated, and the relationship between the mango pixels in the image and its actual weight was analyzed using the statistical regression method. The correlation coefficient of the mango pixels was calculated as 0.9769 (Teoh & Siyaifudin 2007). Furthermore, in studies estimating the weights of adult patients presenting to emergency departments, data were generated by measuring mid-arm length and knee length. The correlation coefficient between the estimated weights of adult patients and actual weights was calculated as 0.89 using the intraclass correlation coefficient. The correlation coefficient between the actual weights and estimates from doctors and nurses was 0.85 and 0.78, respectively (Lin et al. 2009). The age-based weight estimation of Korean children was also performed. The formula used in the study resulted in a success rate of 0.952 (Park et al. 2012).

The objective of this study is to predict the weight of round-shaped fruits and vegetables, drawing inspiration from previous research on live weight prediction in animals. The live body weights of animals are estimated by measuring certain body dimensions. Similarly, machine learning models can predict the weight of vegetables and fruits by analyzing data obtained from their images and using certain criteria. As in the case of animals, the weight estimation of vegetables and fruits without any damage to the product provides convenience in the sale of round-shaped vegetables and fruits in the field, grocery stores and markets where weighing is not possible. Thus, it creates advantageous situations for both producers and consumers by providing convenience in making single or wholesale sales. Simultaneously, estimating the weight of products without handling or damaging them prevents the spread of diseases caused by touching during weighing. This method will help consumer's select rotten or diseased vegetables and fruits because they are lighter than ripe products. It is also a guideline for studies that follow the growth of fruit and vegetables according to their weight.

2. Material and Methods

Figure 1 shows a flow chart of the model developed to predict the weight of round or spherical fruits and vegetables such as watermelons, apples, oranges and tomatoes sold in markets. Precision weighing was used to measure the weight of selected vegetables and fruits. To take pictures of the fruit and vegetables, a device with two arms at different heights was designed and mobile phones were placed on the arms and the pictures were taken at the same distance. Masks were created for the images selected for the training dataset in the segmentation of the images using the U-net architecture. In the segmentation images obtained as the result of U-Net, the pixels containing vegetables and fruits were colored white and the other pixels were black. Furthermore, the area comprising the white pixels from the segmented images was enclosed in a rectangle. New data was obtained by calculating the ratio of white pixels to all pixels and the ratio of the width and height of the rectangle to the width and height of the image. New data were utilized in regression models of machine learning for weight prediction.

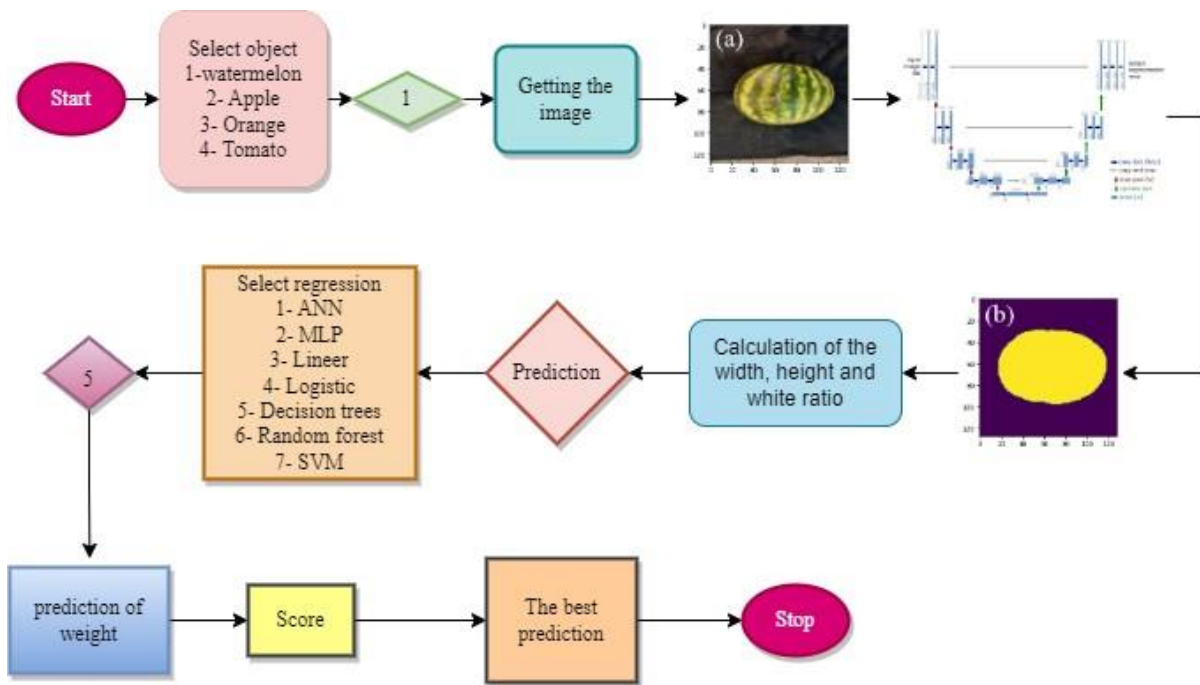


Figure 1- Flow chart of the study

To acquire the fruits and vegetables images, the procedures shown in Figure 2 were followed. Watermelons, apples, oranges, and tomatoes were obtained and weighed with the seller's permission from grocery stores and markets to generate data, as shown in Figure 3, and then images were taken at the same height using a mobile phone placed on the apparatus. The apparatus is designed with two arms and a flat white base on the lower tray. The high arm is designed for taking images of large fruits and vegetables, such as watermelon and melon, and the low arm is designed for taking images of small fruits and vegetables, such

as apples, oranges, and tomatoes. The study analyzed a total of 5000 images from 600 watermelons, 2360 images from 472 tomatoes, 4417 images from 564 apples and 2651 images from 528 tangerines. In the segmentation process with U-Net, 60 images and 60 masks were utilized as the training data, with 40 images employed as the test data. Furthermore, 80% of the data was allocated for training, with the remaining 20% reserved for testing in regression models.

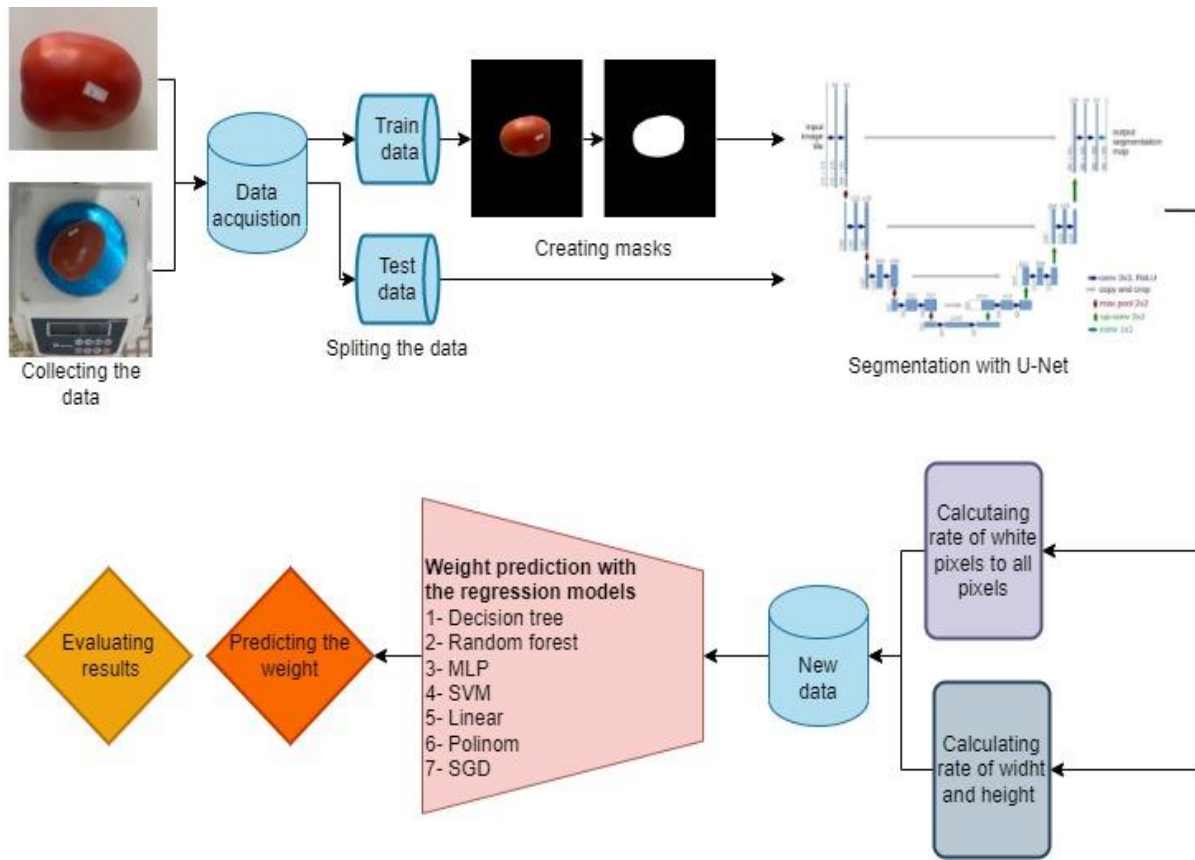


Figure 2- Processes of data acquisition and prediction

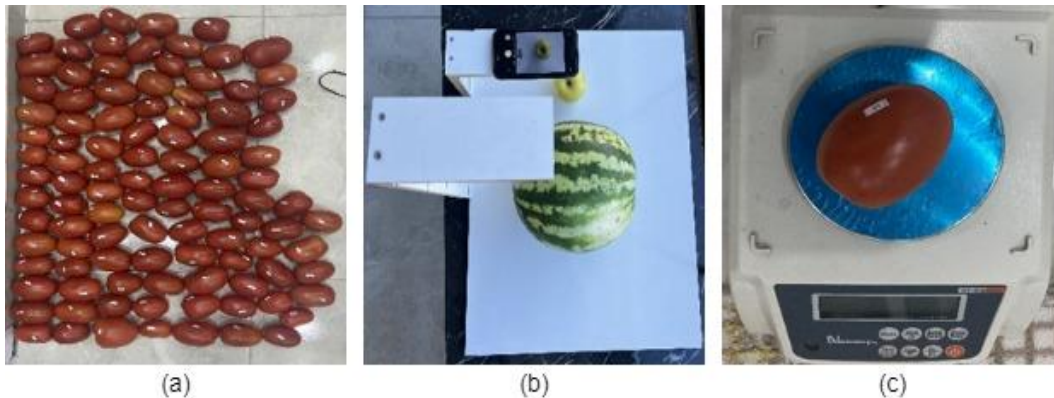


Figure 3- Fruits and vegetables a) tomatoes b) taking the image c) weighing the tomato

2.1. Segmentation of watermelon images with U-Net

Image segmentation is defined as semantic segmentation, which classifies each pixel with semantic labels, sample segmentation, which is based on the segmentation of each object separately, and panoptic segmentation, which combines both segmentations. Semantic segmentation plays a significant role in methods that can divide the image into semantically different objects or parts, which is one of the difficulties in computer vision (Guo et al. 2018). Sample segmentation, on the other hand, solves the object detection problem along with semantic segmentation by assigning labels to different samples of each class. When evaluated for accuracy, the U-Net architecture surpasses traditional segmentation methods. This is specifically important for segmentation methods based on deep CNN (Zhou & Yang 2019).

2.2. Creating a mask

Some of the images were selected for segmentation. Datasets were separated as test and training data in the segmentation with the U-Net architecture. When crafting the image masks utilized for the train data, the background of the image was first erased and the masks were created by coloring the pixels covered by vegetables and fruits as white and the other pixels as black, as shown in Figure 4. The image segmentation was performed using the U-Net architecture, which yields good results with a small number of images shown in Figure 5. The segmentation process was carried out using 100 images, masks of these images and 40 images for testing purposes.

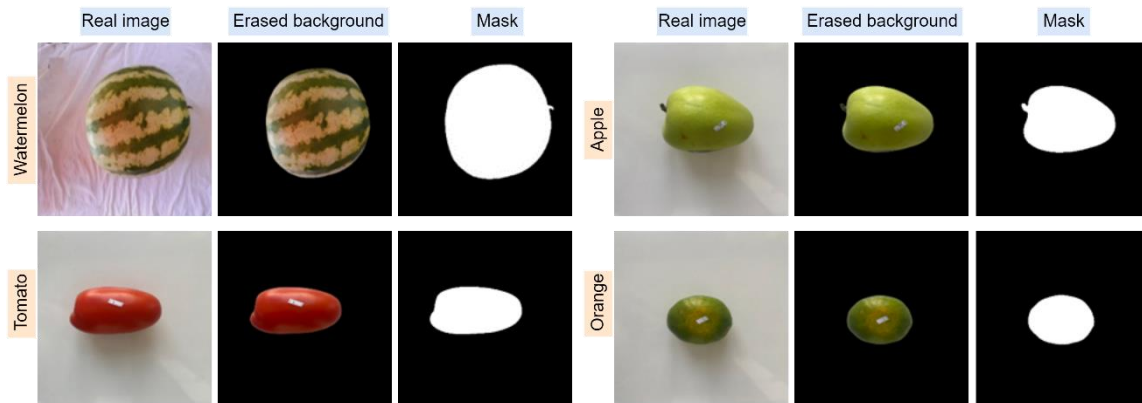


Figure 4- Creating the masks

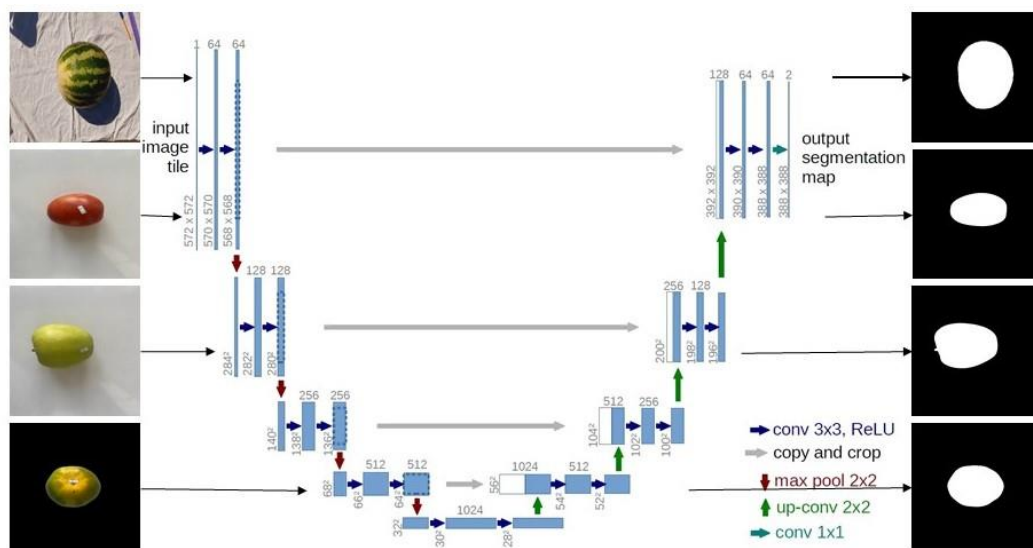


Figure 5- U-Net architecture used in segmentation

2.3. Regression models

The Simple Linear Regression (SLR) is a linear relationship between the independent variable x and the dependent variable y . The line can be accurately described by its y -intercept and slope values. The slope measures the strength of the relationship, while the y -intercept represents the initial position of the regression line (Bangdiwala 2018). The SVM employs a regression model to draw both linear and non-linear lines while maximizing the inclusion of data points. These lines, also known as support vector points, are an essential feature of the model (Wu et al. 2004). In the DT regression model, a random number of nodes and branches at the nodes is used to divide the input data into leaves and branches with consideration for a certain function during training. This enables the regression process to be executed with precision and accuracy (Pekel 2020). The RF is a model produced by training each decision tree on multiple decision trees with different observational data. It is a combination of independent sampling of each tree and making predictions based on the values of the randomly distributed vector of trees with the same distribution. Due to these features, it is applicable to both classification and regression analyses (Breiman 2001). The MLP and ANN are models inspired by the human nerve cell used in fields such as pattern classification, function approach, and dynamic systems. They are based on an information system that multiplies weights on parallel lines connected to all hidden layers of the input layer information, which then passes through the functions used in the hidden layers (Han & Qiao 2013).

2.4. Evaluation criteria

The Mean Squared Error (MSE) is computed as the square of the distance between the actual value and the predicted value (Eq. 1). The Mean Absolute Error (MAE) is a metric that calculates the absolute difference between the actual value and the predicted value (Eq. 2). The Root Mean Squared Error (RMSE) is calculated as the square root of the MSE (Eq. 3). The R^2 is a statistical measure that calculates the degree of closeness between the actual values and the regression line (Eq. 4).

$$MSE = \frac{1}{n} \sum_{i=1}^n (Y_i - \hat{Y}_i)^2 \quad (1)$$

$$MAE = \frac{1}{n} \sum_{i=1}^n |Y_i - \hat{Y}_i| \quad (2)$$

$$RMSE = \sqrt{\frac{1}{n} \sum_{i=1}^n (Y_i - \hat{Y}_i)^2} \quad (3)$$

$$R^2 = 1 - \frac{\frac{1}{n} \sum_{i=1}^n (Y_i - \hat{Y}_i)^2}{\frac{1}{n} \sum_{i=1}^n |Y_i - \hat{Y}_i|} \quad (4)$$

3. Results

3.1. U-Net results

The results of the U-Net segmentation used in this study are shown in Figure 6. A good result of 0.9961 was obtained by using 100 images with their masks. While the accuracy of the training rose from 0.80 to 0.9961 when 100 epochs were employed, not much of an increase was observed after about 50 epochs. Segmentation images were generated using the values acquired during the training process, as shown in Figure 7.

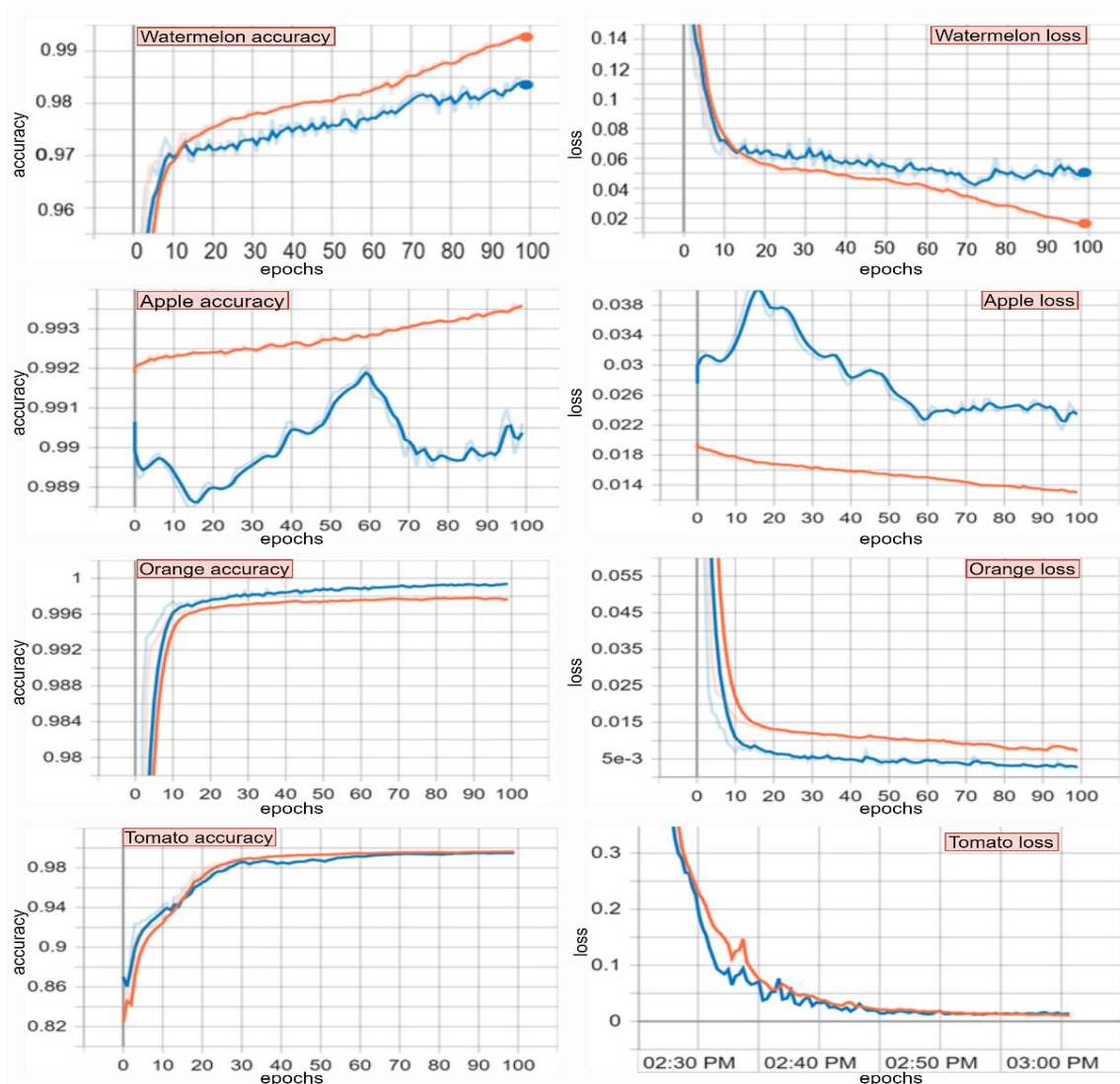


Figure 6- Results of the U-Net train and validation

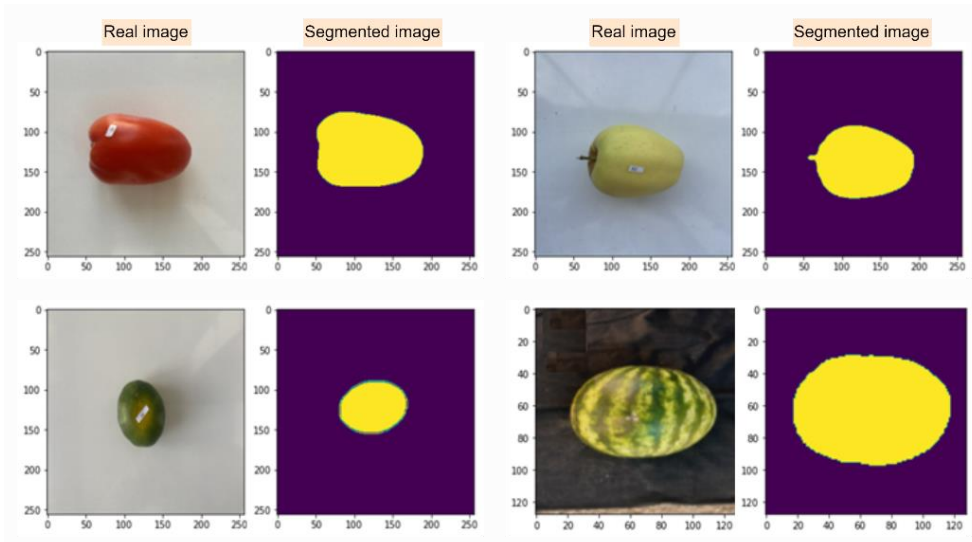


Figure 7- Results of the U-Net segmentation

3.2. Generating data from segmentation images

New data was generated by calculating the ratio of the pixel number of the white in the segmented watermelon images to the total pixel number of each image. Furthermore, by drawing a rectangle over the image shown in Figure 8 that includes the white area, the width rate is calculated as the ratio of the width of the rectangle to the width of the image, and the height rate is calculated as the height of the rectangle to the height of the image. Table 2 presents some of the new data calculated for watermelon. Similarly, these ratios calculated for the watermelon were also calculated for the apple, orange, and tomato.

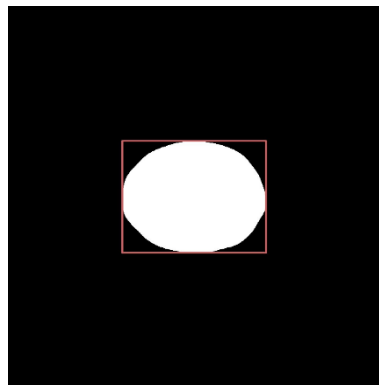


Figure 8- Determination of the image's width, height and ratio of white

Table 1- Pixel ratios obtained from the watermelon images based on the segmentation process

<i>Height</i>	<i>Widht</i>	<i>Ratio of white</i>	<i>Weight</i>
0.372403604	0.445519810	0.139808444	4.885
0.385702246	0.454783085	0.147930963	5.465
0.380525952	0.489560750	0.156355111	6.760
0.472652356	0.470154164	0.171111111	7.300
0.399590102	0.560533784	0.180710667	8.575
0.370586360	0.588517670	0.207366197	9.150
0.410002223	0.632022333	0.225555555	10.055
0.500002233	0.610022340	0.259990526	11.330
0.423666657	0.445569890	0.288002222	12.325
0.571152700	0.558889777	0.329933338	13.708
0.441111223	0.502222256	0.343333333	14.120
...

Figure 9 shows a comparison of the ratios of white, width, and height obtained from watermelon images. To compare the weight data with other data, it was increased the white, width, and height ratios by multiplying them by certain coefficients and evaluated the results by comparing the data on the graphs. When examining the graphs, it was found that the data with a graph

similar to the weight change is the data that was the white ratio. Upon comparing the data, it was apparent that the graphs were not significantly distant from each other, and the correct results will be obtained by using these data in weight prediction.

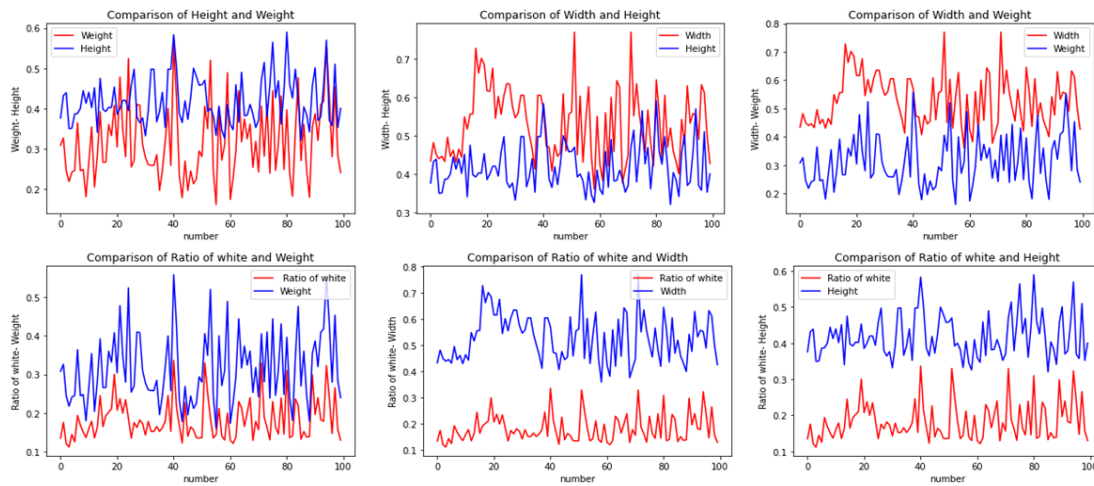


Figure 9- Comparison of the data obtained from the images of the watermelons

3.3. Weight prediction

Weight prediction was performed using regression methods, with the watermelon weights as output data and the ratios obtained from the images as input data. MSE, MAE, RMSE, and R^2 score values were calculated from the training results of each model and added in Table 3. Upon analysis of the regression results, it is evident that decision tree and random forest models show higher training success for weight prediction. The random forest regression model produced the best result, whereas the SGD model yielded the worst outcome, according to the training success. However, the R^2 scores- indicating the percentage success in regression training- were lower in watermelon as opposed to the higher scores obtained in apple, orange, and tomato data training. The findings show that watermelon achieved the lowest success in training, with 91.12%, whereas in training success of apple scored 99.44%, tomato scored 99.89%, and orange scored 99.96%. This low training success for watermelon can be attributed to its weight and the amount of space it occupies in the image, which varies more than other products.

Table 2- Results of regression

Fruit and vegetable	Model	MSE	MAE	RMSE	R^2 score
Watermelon	MLP	2.147	68.383	14.652	0.6794
	SVM	4.071	1.279	20.176	0.3922
	Linear	3.329	110.423	18.742	0.5029
	SGD	3.728	1.371	19.309	0.4433
	DT	0.612	0.234	0.7823	0.9086
	RF	0.637	0.221	0.7982	0.9112
Apple	MLP	59.162	6.012	7.6917	0.8923
	SVM	50.0782	5.6373	7.077	0.9088
	Linear	39.66	4.8932	6.2982	0.9278
	SGD	74.778	6.8857	8.6475	0.8639
	DT	4.5534	0.5128	2.1339	0.9917
	RF	3.0878	0.7917	1.7572	0.9944
Tomato	MLP	19.547	3.0916	4.4209	0.9853
	SVM	244.87	9.344	15.649	0.815
	Linear	35.192	4.4524	5.9596	0.9732
	SGD	222.39	10.3075	14.913	0.8319
	DT	1.6654	0.212	1.2905	0.9987
	RF	1.4368	0.3713	1.1987	0.9989
Orange	MLP	8.331	2.152	2.8864	0.983
	SVM	12.733	2.4505	3.5684	0.974
	Linear	7.759	2.0114	2.786	0.9842
	SGD	28.7058	4.029	5.356	0.9414
	DT	0.2013	0.0817	0.4487	0.9996
	RF	0.2025	0.1946	0.45	0.9996

The graphs shown in Figure 10 were drawn for each model to show the actual and predicted values together and to evaluate the results of the weight predictions made by the regression models. The graphs shown in Figure 10 were drawn for each model

to show the actual and predicted values together and to evaluate the results of the weight predictions made by the regression models. In these graphs, the values on the diagonal line indicate the success of the prediction. The graphs show the weight predictions made by MLP, SVM, Linear, SGD, RF, and DT models for watermelon, apple, orange, and tomato. Although the success rate of predictions in random forest and decision tree models, where values are concentrated on the diagonal line in the graphs, is high, the data is scattered in models such as SGD and SVM, so the success rate is low. Since watermelon has low weight predictions, in the graphs in the first column, the actual and predicted values are scattered around the diagonal line. Because the success rate is high for tomatoes and oranges, the actual and predicted values are concentrated on a diagonal line.

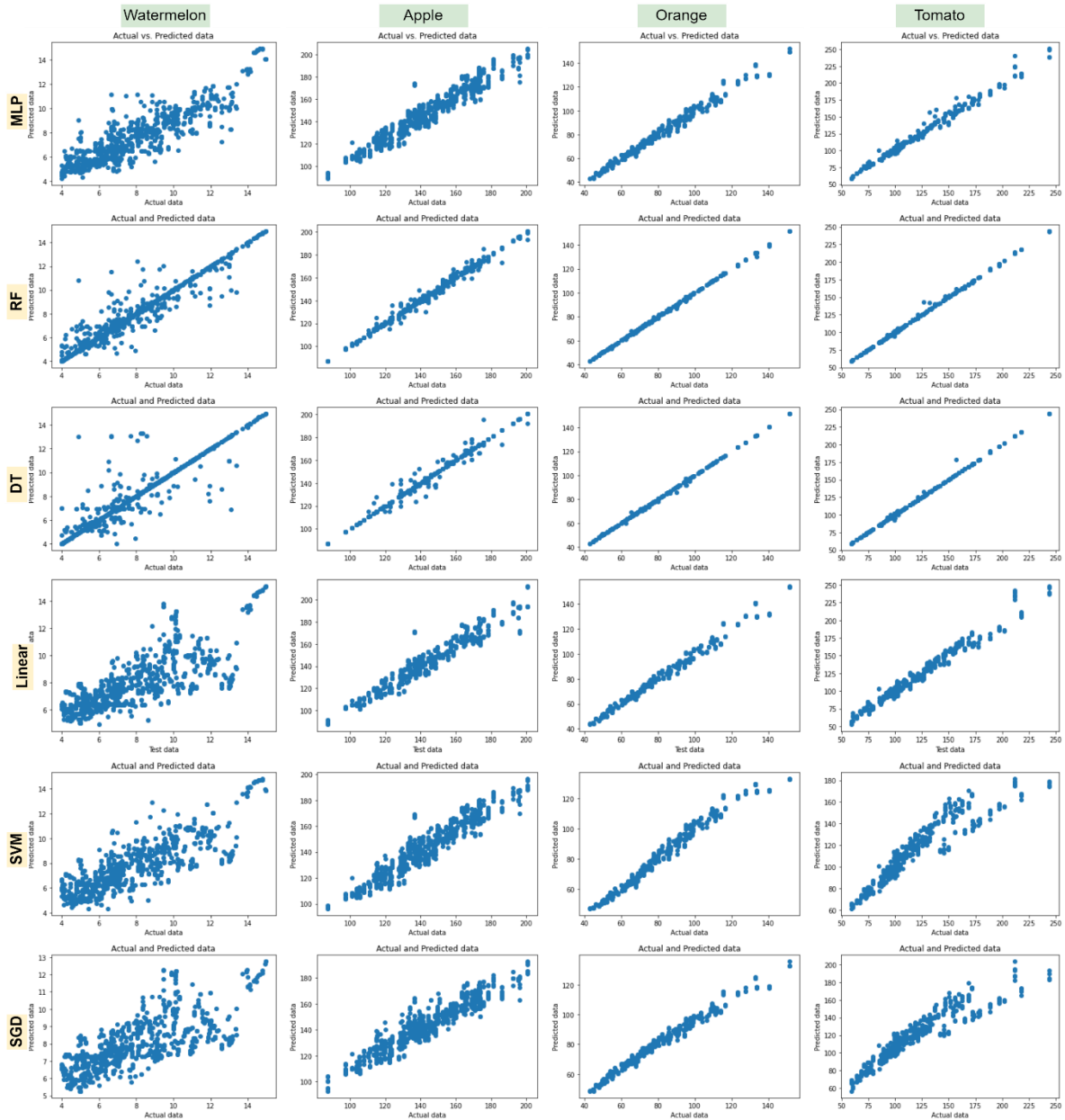


Figure 10- Prediction graphs based on regression results

The graphs shown in Figure 11 were created to compare some weights selected from the test data and the predictions made by the models used in the regression. Graphs were drawn using 1000 data selected from the test data. According to these results, it is seen that the differences in the predictions made in linear models from the actual weights are high, while the differences are low in non-linear models. Findings showed noteworthy disparities between actual weights and predicted weights with the linear models. However, non-linear models showed comparatively lower discrepancies. The graphs display real values in red and predicted values in blue. The graphs where the red color disappears under the blue color are RF and DT models with high prediction success. When analyzing the graphs where the red color increases, the worst predictions were made for watermelon. The linear, SVM, and SGD models were also the worst predictors.

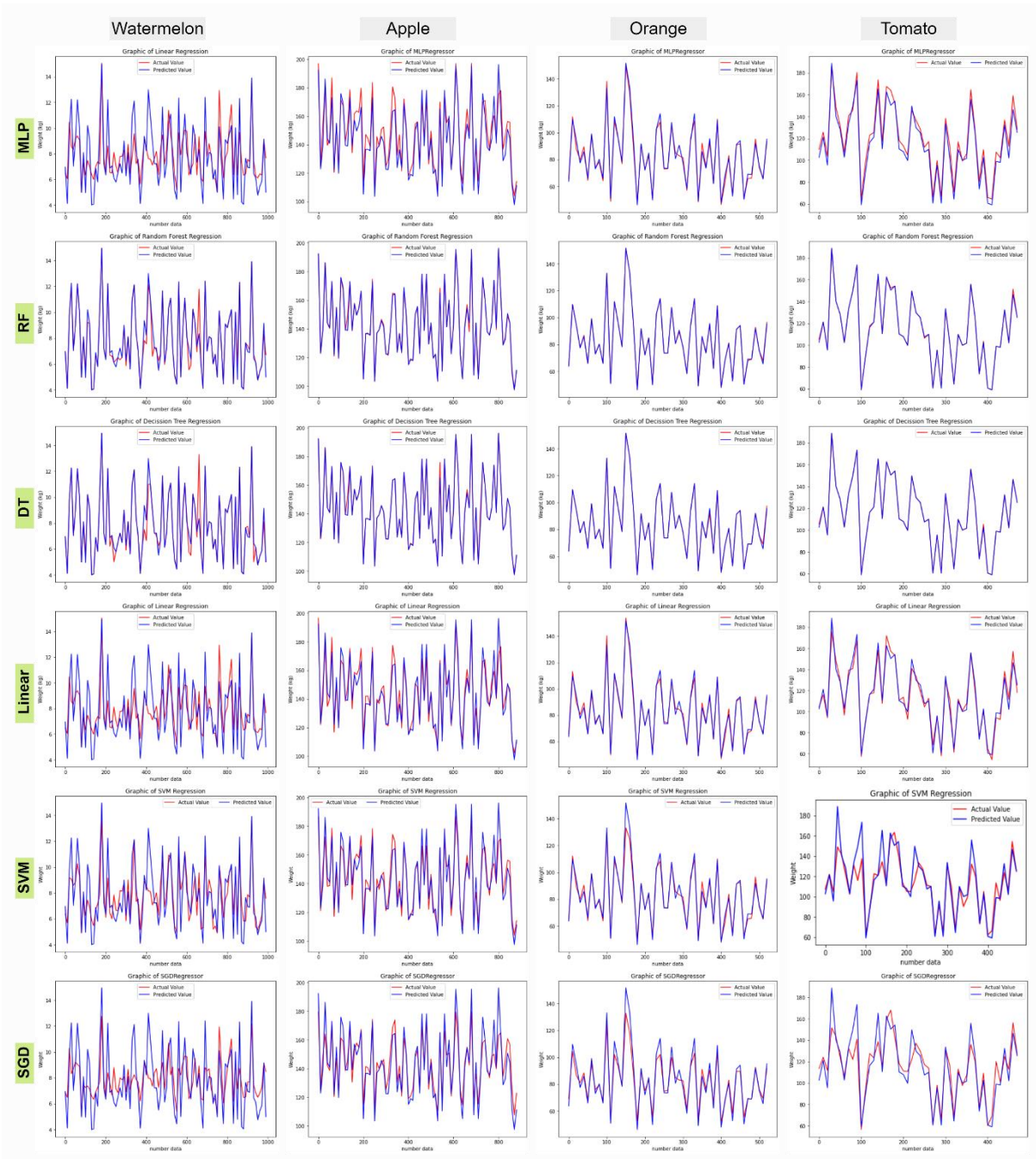


Figure 11- Comparing the predictions derived from the models with the actual results

4. Discussions

In this study, mask images of round-shaped vegetables and fruits were obtained by segmenting images taken at equal distances with a CNN based U-Net architecture. In the segmentation training, the highest success rate was obtained for orange, with 99.96%. When the literature on image segmentation is examined, it is seen that the success rate varies between 70% and 99.88%, with the degree of success depending on the complexity of the process. As the background complexity increases, the success rate of image segmentation decreases. The segmentation result was high due to the clean backgrounds of fruits and vegetables and the presence of a single product in each image. Rudenko et al. (2020) posited that segmentation success may decline when complex images or multiple products are present in the same image. In instances where there are multiple products in the image or the products are overlapping, the mask of the objects may not be fully displayed. In the segmentation and object detection studies of Bargoti & Underwood (2024) and Kang & Chen (2020), the objects in close proximity to the apple image were identified as apples in instances where the apples on the tree were obstructed by leaves and branches. This was achieved through the use of the WS and DasNet-v2 algorithms. By utilizing these algorithms, object detection can be performed in the presence of more than one product in the image. Furthermore, in images where multiple products are displayed together in a greengrocer's aisle or market stalls, the masks of the apples beneath the top apples appear to be missing. With object detection, the missing

masks are displayed as a whole, and weight estimation can be made using the data obtained from these masks. In addition to the images captured at equal distances as in this study, images are also captured with the assistance of a LiDAR sensor and distance sensors (Xu et al. 2024; Jeong et al. 2024). While distance is not a significant factor in images captured at equal distance, it becomes crucial in images obtained through sensor technology. With the advent of applications on mobile devices utilizing sensor technology, consumers will have more expedient access to information regarding the weight of a product by obtaining data from images of the product in various environments, negating the need for equal distance and creating more precise weight estimates. In environments where fruits such as apples, oranges and tomatoes are present, it has been observed that weight estimation can be improved by identifying the fruits and completing the missing ones in cases where the product is not fully visible in the image.

As with the generation of the mask area, width and height ratios, data are generated with features such as the length and width of the actual product, the number of products, the volume and area of the product by immersion in water, and agronomic and phenologic factors (Teoh & Syaifudin 2007; Rad et al. 2015; Naroui Rad et al. 2017). Furthermore, an alternative method for determining the area covered by the product using a point cloud or for obtaining product information by detecting the endpoints of the product has also been developed. The results of this study indicate that not only round-shaped vegetables and fruits, but also non-round products such as radish, soybean, cucumber, and eggplant, can be segmented and various data can be obtained from the images. This allows for the estimation of weight for these products. By using masks of products such as carrots, peppers, aborigines, and bananas, datasets such as area, width, and height ratios can be obtained. Moreover, in this study, data comprising ratios with low values were multiplied by specific numbers, and the consistency of the data was evaluated using graphs. In the estimation of vegetable and fruit weights, studies on small-sized products are typically conducted, whereas there are few studies on the weight of products such as watermelon. Given the variability in the weights of large-sized products, segmentation and weight estimates are often low.

Table 3- Studies on weight prediction

<i>Studies</i>	<i>Obtaining Data</i>	<i>Prediction Model</i>	<i>Score</i>	<i>Predicted Weight</i>
Kamiwaki & Fukuda (2024)	3D image processing	RF	0.95	Radish
Jeong et al. (2024)	Camera and LiDAR	HRNet	0.95	Strawberry
Duc et al. (2023)	Digital image analysis	RF	0.98	Soybean
Xu et al. (2024)	LiDAR	DNN	0.979	Sweetpotato
Nyalala et al. (2019)	Computer vision	RBF-SVM	0.9694	Cherry tomato
Huynh et al. (2020)	Camera	Equal slices	0.967	Cucumber
Ying-Kai et al. (2023)	Computer vision	ANN	0.986	Dragon fruit
Teoh & Syaifudin (2007)	Image processing	Statistical regression	0.9769	Chokanan mango
Xu et al. (2020)	UAV Remote sensing data	ANN	0.8170	Cotton boll
Naroui Rad et al. (2017)	Agronomic and phenologic factor	ANN	0.93	Eggplant
Rad et al. (2015)	Fruit sizes	ANN	0.88	Melon
Faisal et al. (2020)	Computer vision	SVM-Linear	0.84	Date fruit
Our's study	Image processing	RF	0.9996	Orange

Table 3 presents a selection of studies that estimate the weight of various round vegetables and fruits, including watermelon, apple, orange and tomato, as well as products with different shapes. These studies are achieved by obtaining data from image or real dimensions. The weight estimation model employed in this study allows for the estimation of fruit weight in studies investigating the weight of ripe fruit, as well as in studies following the development of the product. The studies yielded a success rate of between 84% (Xu et al. 2020) and 99% (Ying-Kai et al. 2023) in predicting fruit development and mature fruit weight. A comparison of the success rates of weight predictions obtained for each product in the study with those presented in the table reveals that satisfactory results have been achieved. It has been demonstrated that machine learning models are more successful at making predictions in studies with less data. In this study, machine learning models such as RF, MLP, DT, Linear, SGD and SVM were employed due to the lack of a large dataset and limited variety. The results indicated that the RF and DT models exhibited the highest prediction success rates for all products. Conversely, the SVM and linear models demonstrated the lowest prediction accuracy. The results of the RF model are particularly useful for predicting the weight of fruits and vegetables. While a small number of regression models were used in many studies, six models were used in this study, and the most appropriate prediction model was determined. Thus, the results of this study demonstrate that nonlinear RF and DT models achieve higher success rates than linear models in proportion to the diversity and complexity of the product in the image. The developed model has shown superior prediction performance by selecting the model with the highest success rate.

5. Conclusions

In this study, the model was developed to predict the weights of fruits and vegetables such as watermelons, apples, oranges and tomatoes using data obtained from their images taken at equal distances. To collect the images, products were purchased from markets and greengrocers, their images were taken and weighed, and their weights were recorded. The images were segmented utilizing the U-Net architecture, the area covered by the product was colored white, while the other pixels were colored black. Three new data were generated for each image such as the ratio of white pixels to all pixels, the ratio of the width of the rectangle to the width of the image when white pixels are contained in a rectangle, and the ratio of the height of the rectangle to the height

of the image. Weights were predicted using the data obtained from the image. In the regression models used in the model, good predictions were made with high success rates in random forest and decision tree models, while low predictions were made with low success rates in models such as linear and SGD. The best prediction success percentages were 91.12% for watermelon, 99.14% for apple, 99.96% for orange, and 99.89% for tomato. According to these results, nonlinear models were more successful in predicting weights than linear models. In addition, it has been observed that linear models in regression and classification models have lower scores than models such as non-linear ANN, DT and RF. With live body weight prediction, the body weight of the animal is known before the animal is disturbed and slaughtered. Similarly, non-destructive weight estimation of fruits and vegetables can be performed without damaging or cutting them. It is also possible to predict the weight of fruits and vegetables such as watermelons, apples, oranges, and tomatoes in cases where it is not possible to weigh it, providing convenience in the fields or in environments where there are no scales. At the same time, it is predicted that the estimated weight of the watermelons in the watermelon fields can be used in bargaining, such as selling products on the field. Similarly, at the time of harvest, tomatoes in the field and apples and oranges on the trees can be sold wholesale without weighing. Furthermore, given the recent surge in infectious diseases, the transmission of viruses through hand-to-hand contact during product selection and weighing will be minimized.

References

- Akkol S, Akilli A & Cemal I (2017). Comparison of artificial neural network and multiple linear regression for prediction of live weight in hair goats. *Yyu J. Agric. Sci* 27: 21-29. DOI: 10.29133/yyutbd.263968
- Alzubaidi L, Zhang J, Humaidi A J, Al-Dujaili A, Duan Y, Al-Shamma O, Santamaria J, Fadhel M A, Al-Amidie M & Farhan L (2021). Review of deep learning: Concepts, CNN architectures, challenges, applications, future directions. *Journal of big Data* 8(1): 1-74. DOI: 10.1186/s40537-021-00444-8
- Babajide O, Hissam T, Anna P, Anatoliy G, Astrup A, Alfredo Martinez J, Oppert J M & Sørensen T I (2020). A machine learning approach to short-term body weight prediction in a dietary intervention program. *In Computational Science-ICCS 2020: 20th International Conference, Proceedings, Part IV 20* (pp. 441-455). DOI: 10.1007/978-3-030-50423-6_33
- Bangdiwala S I (2018). Regression: simple linear. *International journal of injury control and safety promotion* 25(1): 113-115. DOI: 10.1080/17457300.2018.1426702
- Barbole D K, Jadhav P M & Patil S B (2021). A review on fruit detection and segmentation techniques in agricultural field. *In International Conference on Image Processing and Capsule Networks* (pp. 269-288). Springer, Cham. DOI: 10.1007/978-3-030-84760-9_24
- Bargoti S & Underwood J P (2017). Image segmentation for fruit detection and yield estimation in apple orchards. *Journal of Field Robotics* 34(6): 1039-1060. DOI: 10.1002/rob.21699
- Breiman L (2001). Random forests. *Machine learning*, 45: 5-32. DOI: 10.1023/A:1010933404324
- Castro C A D O, Resende R T, Kuki K N, Carneiro V Q, Marcatti G E, Cruz C D & Motoike S Y (2017). High-performance prediction of macauba fruit biomass for agricultural and industrial purposes using Artificial Neural Networks. *Industrial Crops and Products*, 108: 806-813. DOI: 10.1016/j.indcrop.2017.07.031
- Chicchón Apaza M Á, Monzón H M B & Alcarria R (2020). Semantic segmentation of weeds and crops in multispectral images by using a Convolutional Neural Networks based on u-net. *In International Conference on Applied Technologies* (pp. 473-485). Springer, Cham. DOI: 10.1007/978-3-030-42520-3_38
- Cornelis C, Deschrijver G & Kerre E E (2006). Advances and challenges in interval-valued fuzzy logic. *Fuzzy sets and systems*, 157(5): 622-627. DOI: 10.1016/j.fss.2005.10.007
- Duc N T, Ramlal A, Rajendran A, Raju D, Lal S K, Kumar S, Sahoo R N & Chinnusamy V (2023). Image-based phenotyping of seed architectural traits and prediction of seed weight using machine learning models in soybean. *Frontiers in Plant Science*, 14: 1206357. DOI: 10.3389/fpls.2023.1206357
- Faisal M, Albogamy F, Elgibreen H, Algabri M & Alqershi F A (2020). Deep learning and computer vision for estimating date fruits type, maturity level, and weight. *IEEE Access*, 8: 206770-206782. DOI: 10.1109/ACCESS.2020.3037948
- Fernandes A F, Turra E M, de Alvarenga É R, Passafaro T L, Lopes F B, Alves G F, Singh V & Rosa G J (2020). Deep Learning image segmentation for extraction of fish body measurements and prediction of body weight and carcass traits in Nile tilapia. *Computers and electronics in agriculture*, 170: 105274. DOI: 10.1016/j.compag.2020.105274
- Friha O, Ferrag M A, Shu L, Maglaras L & Wang X (2021). Internet of Things for the Future of Smart Agriculture: A Comprehensive Survey of Emerging Technologies. *IEEE/CAA J. Autom. Sinica*, 8(4): 718-752. DOI: 10.1109/JAS.2021.1003925
- Gondchawar N & Kawitkar R S (2016). IoT based smart agriculture. *International Journal of advanced research in Computer and Communication Engineering*, 5(6): 838-842. DOI: 10.1088/1757-899X/1212/1/012047
- Guo Y, Liu Y, Georgiou T & Lew M S (2018). A review of semantic segmentation using deep neural networks. *International journal of multimedia information retrieval*, 7(2): 87-93. DOI: 10.1007/s13735-017-0141-z
- Han H G & Qiao J F (2013). A structure optimisation algorithm for feedforward neural network construction. *Neurocomputing*, 99: 347-357. DOI: 10.1016/j.neucom.2012.07.023
- Huynh T, Tran L & Dao S (2020). Real-time size and mass estimation of slender axi-symmetric fruit/vegetable using a single top view image. *Sensors*, 20(18): 5406. DOI: 10.3390/s20185406
- Jeong H, Moon H, Jeong Y, Kwon H, Kim C, Lee Y, Yang S M & Kim S (2024). Automated Technology for Strawberry Size Measurement and Weight Prediction Using AI. *IEEE Access*. 12: 14157-14167. DOI: 10.1109/ACCESS.2024.3356118
- Kang H & Chen C (2020). Fruit detection, segmentation and 3D visualisation of environments in apple orchards. *Computers and Electronics in Agriculture*, 171: 105302. DOI: 10.1016/j.compag.2020.105302
- Kassim M R M (2020). IoT applications in smart agriculture: Issues and challenges. *In 2020 IEEE conference on open systems (ICOS)* (pp. 19-24). IEEE. DOI: 10.1109/ICOS50156.2020.9293672
- Kamiwaki Y & Fukuda S (2024). A Machine Learning-Assisted Three-Dimensional Image Analysis for Weight Estimation of Radish. *Horticulturae*, 10(2): 142. DOI: 10.3390/horticulturae10020142

- Lee C Y (2023). Fruit Weight Predicting by Using Hybrid Learning. *In International Conference on Technologies and Applications of Artificial Intelligence*, (pp. 81-91). Singapore. DOI: 26912554
- Li J, Sarma K V, Ho K C, Gertych A, Knudsen B S & Arnold C W (2017). A multi-scale u-net for semantic segmentation of histological images from radical prostatectomies. *In AMIA Annual Symposium Proceedings*. (pp. 1140). American Medical Informatics Association. DOI: PMC5977596
- Lin B W, Yoshida D, Quinn J & Strehlow M (2009). A better way to estimate adult patients' weights. *The American journal of emergency medicine*, 27(9): 1060-1064. DOI: 10.1016/j.ajem.2008.08.018
- Mahesh B (2020). Machine learning algorithms-a review. *International Journal of Science and Research (IJSR)*, 9: 381-386. DOI: 10.21275/ART20203995
- Naroui Rad M R, Ghalandarzahi A & Koochpaygani J A (2017). Predicting eggplant individual fruit weight using an artificial neural network. *International Journal of Vegetable Science*, 23(4): 331-339. DOI: 10.1080/19315260.2017.1290001
- Nyalala I, Okinda C, Nyalala L, Makange N, Chao Q, Chao L, Yousaf K & Chen K (2019). Tomato volume and mass estimation using computer vision and machine learning algorithms: Cherry tomato model. *Journal of Food Engineering*, 263: 288-298. DOI: 10.1016/j.jfoodeng.2019.07.012
- O'Grady M J, Langton D & O'Hare G M P (2019). Edge computing: A tractable model for smart agriculture. *Artificial Intelligence in Agriculture*, 3: 42-51. DOI: 10.1016/j.iaia.2019.12.001
- Ozkaya S (2013). The prediction of live weight from body measurements on female Holstein calves by digital image analysis. *The Journal of Agricultural Science*, 151(4): 570-576. DOI: 10.1017/S002185961200086X
- Park J, Kwak Y H, Jung J Y, Lee J H, Jang H Y, Kim H B & Hong K J (2012). A new age-based formula for estimating weight of Korean children. *Resuscitation*, 83(9): 1129-1134. DOI: https://doi.org/10.1016/j.resuscitation.2012.01.023
- Pathan M, Patel N, Yagnik H & Shah M (2020). Artificial cognition for applications in smart agriculture: A comprehensive review. *Artificial Intelligence in Agriculture*, 4: 81-95. DOI: 10.1016/j.iaia.2020.06.001
- Pekel E (2020). Estimation of soil moisture using decision tree regression. *Theoretical and Applied Climatology*, 139(3-4): 1111-1119. DOI: 10.1007/s00704-019-03048-8
- Rad M R N, Fanaei H R & Rad M R P (2015). Application of Artificial Neural Networks to predict the final fruit weight and random forest to select important variables in native population of melon (*Cucumis melo* L.). *Scientia Horticulturae*, 181: 108-112. DOI: https://doi.org/10.1016/j.scienta.2014.10.025
- Rozario L J, Rahman T & Uddin M S (2016). Segmentation of the region of defects in fruits and vegetables. *International Journal of Computer Science and Information Security*, 14(5): 399-406. https://www.researchgate.net/publication/304253402
- Rudenko O, Megel Y, Bezsonov O & Rybalka A (2020). Cattle breed identification and live weight evaluation on the basis of machine learning and computer vision. *In CMIS* (pp.939-954). https://eur-ws.org/Vol-2608/paper70.pdf
- Teoh C C & Syaifudin A M (2007). Image processing and analysis techniques for estimating weight of Chokanan mangoes. *Journal of Tropical Agriculture and Food Science*, 35(1): 183. DOI: http://jtafs.mardi.gov.my/jtafs/35-1/Chokanan%20mangoes.pdf
- Xiao J & Zhou Z (2020). Research progress of RNN language model. *In 2020 IEEE International Conference on Artificial Intelligence and Computer Applications (ICAICA)* (pp. 1285-1288). IEEE. DOI: 10.1109/ICAICA50127.2020.9182390
- Xu J, Lu Y, Olaniyi E & Harvey L (2024). Online volume measurement of sweetpotatoes by A LiDAR-based machine vision system. *Journal of Food Engineering*, 361: 111725. DOI: 10.1016/j.jfoodeng.2023.111725
- Xu W, Yang W, Chen S, Wu C, Chen P & Lan Y (2020). Establishing a model to predict the single boll weight of cotton in northern Xinjiang by using high resolution UAV remote sensing data. *Computers and Electronics in Agriculture*, 179: 105762. DOI: https://doi.org/10.1016/j.compag.2020.105762
- Wu C H, Ho J M & Lee D T (2004). Travel-time prediction with support vector regression. *IEEE transactions on intelligent transportation systems*, 5(4): 276-281. DOI: 10.1109/TITS.2004.837813
- Yan Q, Ding L, Wei H, Wang X, Jiang C & Degen A (2019). Body weight estimation of yaks using body measurements from image analysis. *Measurement*, 140: 76-80. DOI: 10.1016/j.measurement.2019.03.021
- Ying-kai L, Feng-nan S, Qiao C, Ming-wei X, Chen-di L, Wen-tao L & Xue-cheng Z (2023). Dragon fruit weight estimation based on machine vision and machine learning. *Food and Machinery*, 39(7): 99-103. DOI: https://www.ifoodmm.cn/journal/vol39/iss7/15/
- Yu Y, Si X, Hu C & Zhang J (2019). A review of recurrent neural networks: LSTM cells and network architectures. *Neural computation* 31(7): 1235-1270. DOI: 10.1162/neco_a_01199
- Zhou X Y & Yang G Z (2019). Normalization in training U-Net for 2-D biomedical semantic segmentation. *IEEE Robotics and Automation Letters*, 4(2): 1792-1799. DOI: 10.1109/LRA.2019.2896518



Copyright © 2024 The Author(s). This is an open-access article published by Faculty of Agriculture, Ankara University under the terms of the [Creative Commons Attribution License](https://creativecommons.org/licenses/by/4.0/) which permits unrestricted use, distribution, and reproduction in any medium or format, provided the original work is properly cited.